NaTAA concentration in DMSO-d_6 is decreased, are attributed to methyl groups near carbon–sulfur and carbon–oxygen bonds, respectively, in the trans isomer. Very little ion pairing would occur involving this isomer. The γ-proton signal to high field is assigned to the cis isomer, whereas the corresponding low field signal, which remains in dilute solutions, is attributed to essentially uncomplexed *trans*-TAA. Both the conductance and pmr data show that at a given concentration in DMSO solution dissociation is greater for the potassium salt than for the sodium salt.

The pmr spectra for four different 0.2 *M* NaTAA solutions are compared in Figure 6. The positions and intensities of the proton signals in deuterium oxide and methanol solutions exhibit the same type of concentration dependence as that observed in DMSO-d_6 solutions (Table VIII) and analogous assignments are suggested. In pyridine, only the methyl and vinyl proton peaks attributable to uncomplexed TAA^- are observed in 0.2–0.05 *M* NaTAA solutions.

Acknowledgments. We thank Dr. J. Ellern for critical comments. O. S. thanks the National Research Council of Canada for a postdoctoral fellowship (1970–1972). This research was supported by the National Science Foundation and the National Research Council of Canada.

Single-Crystal Structure and 5.0°K Polarized Electronic Spectra of Bis(monothioacetylacetonato)nickel(II). Far-Infrared and Raman Spectra of Bis(monothioacetylacetonato)metal(II) Complexes

Olavi Siiman, Donald D. Titus, Charles D. Cowman, James Fresco, and Harry B. Gray*

Contribution No. 4798 from the Arthur Amos Noyes Laboratory of Chemical Physics, California Institute of Technology, Pasadena, California 91109, and the Department of Chemistry, McGill University, Montreal 110, Quebec, Canada. *Received July 19, 1973*

Abstract: A single-crystal X-ray structure of bis(monothioacetylacetonato)nickel(II) has been completed. The crystals are orthorhombic, space group P_{bca}, with eight molecules per unit cell: $a = 13.301$ (3), $b = 16.418$ (3), $c = 11.468$ (3) Å; $V = 2505$ (1) Å^3; $\rho_o = 1.52$ (2) and $\rho_c = 1.533$ g/cm^3. Diffractometer data were collected using Cu Kα radiation, and the structure was refined by full-matrix least-squares methods with anisotropic thermal parameters for all but the hydrogen atoms to a final $R = 0.072$ for 1676 independent reflections. The molecule is very nearly planar with a cis configuration of sulfur atoms about the nickel atom. Far-infrared and Raman spectra of Ni(II), Pd(II), Zn(II), and Cd(II) bis(monothioacetylacetonates) were recorded between 700 and 100 cm^{-1} Normal coordinate analyses for the Ni(II) and Pd(II) complexes were made, assuming a C_{2v} 1 : 2 metal–ligand model. Bands attributable to M–S stretching vibrations occur at 251 and 194 cm^{-1} in $Ni(TAA)_2$, 224 and 173 cm^{-1} in $Pd(TAA)_2$, 273 and 197 cm^{-1} in $Zn(TAA)_2$, and 245 and 180 cm^{-1} in $Cd(TAA)_2$. The polarized single crystal absorption spectra of $Ni(TAA)_2$ at 5.0°K have been measured between 750 and 400 nm. The low intensity band at 630 nm is slightly π polarized, and is assigned $^1A_1 \rightarrow {}^1B_1$ ($d_{xz} \rightarrow d_{xy}$). Moderately intense features in the 500–400 nm region are assigned to $d \rightarrow b_1\pi^*$ and $d \rightarrow a_2\pi^*$ charge transfer transitions, based on the observed polarizations.

A wide variety of metal complexes of monothio-β-diketonates have been synthesized recently.[1] As cis and trans isomers are possible for both bis-planar and tris-octahedral metal monothio-β-diketonates, structural data are essential for any detailed interpretation of vibrational and electronic spectra. An early report[2] on bis(monothio-β-diketonates) alluded solely to a trans-planar configuration; however, X-ray investigation[3] of bis(monothiodibenzoylmethanato)palladium(II) revealed a cis planar arrangement about palladium. Further, pmr evidence[4] has indicated that tris(monothio-β-diketonato)cobalt(III) and -vanadium(III) exist exclusively as the cis (facial) isomers.

We have carried out an extensive investigation of the structural and spectroscopic properties of several bis(monothioacetylacetonato)metal(II) complexes, hereafter denoted $M(TAA)_2$, in an effort to provide a foundation for electronic structural discussion. In this paper we report complete X-ray crystallographic results and polarized single-crystal electronic spectra at 5°K for $Ni(TAA)_2$, as well as detailed analyses of the vibrational spectra of the $(TAA)_2$ complexes of Zn(II), Cd(II), Ni(II), and Pd(II).

Experimental Section

The preparation of $Zn(TAA)_2$, $Cd(TAA)_2$, $Ni(TAA)_2$, and Pd-

* Address correspondence to this author at the California Institute of Technology.

(1) (a) H. Cox and J. Darken, *Coord. Chem. Rev.*, 7, 29 (1971); (b) S. E. Livingstone, *ibid.*, 7, 59 (1971).

(2) S. H. H. Chaston and S. E. Livingstone, *Aust. J. Chem.*, **20**, 1079 (1967).

(3) E. A. Shugam, L. M. Shkol'nikova, and S. E. Livingstone, *Zh. Strukt. Khim.*, **8**, 550 (1967).

(4) R. H. Holm, D. H. Gerlach, J. G. Gordon, and M. C. McNamee, *J. Amer. Chem. Soc.*, **90**, 4184 (1968).

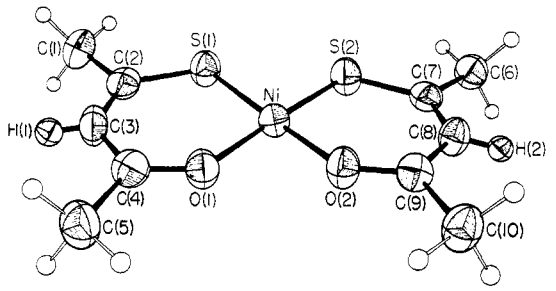

Figure 1. Perspective view of the $Ni(SC(CH_3)CHC(CH_3)O)_2$ molecule. Thermal ellipsoids are drawn at the 50% probability level.

$(TAA)_2$ was accomplished by a previously described method.[5] $Ni(TAA\text{-}d)_2$ was prepared by shaking a solution of monothioacetylacetone-d_2 in $CDCl_3$ with nickel(II) acetate in D_2O. The product was crystallized from the $CDCl_3$ layer after drying over anhydrous $MgSO_4$. It was determined to be about 60% deuterated at the γ-carbon proton position from a pmr spectrum in $CDCl_3$. Monothioacetylacetone-d_2 was prepared by acidifying monothioacetylacetonatosodium(I)[5] with deuterium chloride. The deuterated ligand was extracted into carbon tetrachloride, dried over anhydrous $MgSO_4$, and concentrated. Single crystals of $Ni(TAA)_2$ suitable for X-ray study were grown by vacuum sublimation at ~160°. A clear epoxy cement was used to mount the dark red-brown crystals on thin glass fibers.

Infrared spectra were recorded using Perkin-Elmer Model 521, 225, and 301 spectrophotometers. Frequency readings were calibrated with polystyrene film and water vapor. Potassium bromide and cesium bromide pellets and Nujol mulls between polyethylene windows were prepared for solid-state spectra. Raman spectra of powdered solids of $Pd(TAA)_2$, $Zn(TAA)_2$, and $Cd(TAA)_2$ were recorded with Jarrell-Ash 25-300 and Cary 81 spectrophotometers. The 647.1-nm Kr and the 632.8-nm Ne emission lines were used. Frequency shifts were calibrated with benzene and carbon tetrachloride. The Raman spectrum of $Ni(TAA)_2$ was obtained on a Jarrell-Ash 25-400 spectrophotometer (647.1-nm Kr) utilizing a rotating metal sample holder with a circular groove packed with potassium bromide powder and then with powdered $Ni(TAA)_2$.

Electronic spectra were recorded on a Cary 17 spectrophotometer. Single crystals of $Ni(TAA)_2$ suitable for optical spectroscopy varied in thickness from 3 to 50 μ and had cross sections of about 2×3 mm^2. These crystals were grown on quartz disks by slow evaporation of acetone solutions. The light brown flakes of $Ni(TAA)_2$ were found to have the same space group and cell dimensions as the dark, octahedral-shaped crystals used for the X-ray structure. Extinction directions for the rectangular (010) crystal face were along the c axis, the long axis of the flake, and along the a axis. Liquid helium temperature polarized optical spectra were obtained using an Andonian Associates liquid helium dewar placed in the sample beam following a double-Glan, air-spaced calcite polarizing prism. Spectra were obtained for light polarized along the extinction directions of the crystal.

Collection and Reduction of X-Ray Data. $Ni(TAA)_2$ crystallizes in the orthorhombic system; Weissenberg and precession photographs of the $h0l$, $hk0$, and $0kl$ zones revealed the set of systematic absences uinque for space P_{bca}. The unit cell data are given in Table I.

An irregular polyhedron varying in thickness between 0.12 and 0.07 mm was chosen for intensity data collection. The crystal was mounted with its [101] axis parallel to the ϕ axis of the diffractometer. A Datex-automated General Electric quarter-circle diffractometer was employed for intensity measurements; nickel-filtered copper radiation was used because of the relatively large cell. The intensities were recorded at a scan rate of 1°/min with a symmetrical θ–2θ scan which varied from 2 to 4° over the 2θ range of 4–120°. Background counts of 40 sec each were taken at the extremes of each scan. Three check reflections were monitored periodically throughout the data collection; an average intensity reduction of 2% was noted for these reflections at the completion of the determination.

Table I. Unit Cell Data for $Ni(TAA)_2$[a]

a = 13.301 (3) Å	Orthorhombic, space group P_{bca}
b = 16.418 (3) Å	M = 289.06 Z = 8
c = 11.469 (3) Å	V = 2505 (1) Å^3
ρ_o = 1.52 (2)	ρ_c = 1.533 g/cm^3 μ(Cu Kα) = 49 cm^{-1}

[a] The cell dimensions were obtained from a least-squares refinement of 2θ values of 11 high-angle reflections centered on the diffractometer.

A total of 1849 independent intensities were recorded in eight sets. The reflections in each set were scaled to an arbitrary $|F|$ (chosen for one of the check reflections) which was held constant for all of the data sets. Lorentz and polarization corrections were made, but there was no attempt to correct for absorption. Transmission factors for the crystal varied from 0.56 to 0.71. All reflections which were observed to have zero or negative intensities were assigned an $|F|$ of zero with a zero weight. The solution and refinement of the structure were carried out on the basis of the 1676 nonzero reflections which remained. The $|F|$ values were put on an approximately absolute scale with the use of a Wilson plot. Nonhydrogen[6] and hydrogen[7] atomic scattering factors were taken from standard sources. The scattering factors of Ni and S were corrected for the real part of anomalous dispersion using Cromer's values.[8]

All crystallographic computations were performed under the CRYM system.[9]

Solution and Refinement of the Structure. The positions of the nickel and sulfur atoms were determined from a three-dimensional, sharpened Patterson map. Introduction of the positional parameters of these atoms along with an overall thermal parameter into a structure factor calculation resulted in an R index $(\Sigma||F_o| - |F_o||/\Sigma|F_o|)$ of 0.45. Two successive structure factor calculations interspersed with Fourier syntheses revealed the locations of all of the remaining nonhydrogen atoms.

The model thus obtained was refined by the method of full-matrix least squares. The function minimized was $\Sigma w(|F_o|^2 - |F_c|^2)^2$, where $w = 1/\sigma^2(F_o^2)$. After three cycles of least-squares refinement, in which all atoms were allowed to vibrate anisotropically, the R value stood at 0.080. A difference Fourier map was calculated, revealing the positions of the hydrogen atoms attached to the γ-carbon atoms.

The diffuse character of the electron density about the methyl carbon atoms indicated disorder in the methyl hydrogen atom positions. Assuming a staggered conformation with respect to the γ-carbon atom, positions for the methyl hydrogen atoms were calculated using a tetrahedral carbon model with a C–H bond distance of 1.09 Å. The derived positional parameters of the hydrogen atoms were included as fixed contributions in the subsequent refinements; each hydrogen atom was assigned an isotropic thermal parameter of 6 Å^2. The positional and isotropic thermal parameters of the two hydrogen atoms attached to the γ-carbon atoms were allowed to refine in the final three cycles of least-squares refinement. The final R index was 0.072, and the final error in an observation of unit weight was 1.5. A list of the observed and calculated structure factors is available.[10]

Description of the Molecular Structure

Bis(monothioacetylacetonato)nickel(II) crystallizes as discrete monomers in which the nickel atom is situated in an approximately square-planar environment. A perspective drawing of a molecule of $Ni(TAA)_2$ is shown in Figure 1. The stereochemistry is cis, as in the closely related compound $Pd(C_6H_5COCHCSC_6H_5)_2$.[3] A stereoscopic view of the orientation of $Ni(TAA)_2$ molecules within the unit cell is shown in Figure 2. The shortest Ni–Ni distance, 4.393 Å, is between inversion-related molecules which have their planes parallel to each other. These two molecules are

(5) O. Siiman and J. Fresco, *J. Chem. Phys.*, **54**, 734 (1971).

(6) H. P. Hanson, F. Herman, J. D. Lea, and S. Skillman, *Acta Crystallogr.*, 17, 1040 (1964).

(7) R. F. Stewart, E. R. Davidson, and W. T. Simpson, *J. Chem. Phys.*, **42**, 3175 (1965).

(8) D. T. Cromer, *Acta Crystallogr.*, **18**, 17 (1965).

(9) D. J. Duchamp, Paper B-14, American Crystallographic Association Meeting, Bozeman, Mont., 1964, p 29.

(10) See paragraph at end of paper regarding supplementary material.

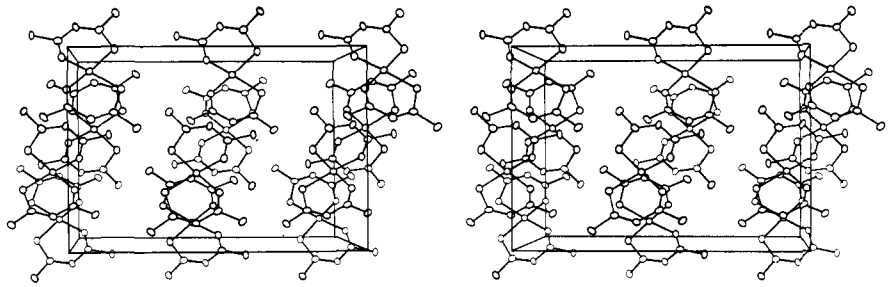

Figure 2. A stereoscopic packing diagram in a unit cell of $Ni(SC(CH_3)CHC(CH_3)O)_2$. The horizontal axis is b and the vertical is c; the origin of the cell is in the upper left rear corner.

Table II. Positional and Thermal Parameters of Bis(monothioacetylacetonato)nickel(II)[a]

Atom	x	y	z	β_{11}	β_{22}	β_{33}	β_{12}	β_{13}	β_{23}
Ni	10,071 (7)	7104 (5)	11,261 (8)	440 (6)	279 (4)	601 (7)	30 (9)	103 (12)	37 (11)
S(1)	574 (1)	1787 (1)	2,054 (1)	62 (1)	31 (1)	72 (1)	4 (1)	25 (2)	−4 (2)
S(2)	1,793 (1)	1531 (1)	−3 (1)	66 (1)	28 (1)	88 (1)	−2 (2)	46 (2)	1 (2)
O(1)	282 (3)	−26 (2)	2,064 (3)	58 (3)	32 (2)	66 (3)	−3 (4)	28 (6)	−1 (4)
O(2)	1,453 (3)	−250 (2)	407 (3)	60 (3)	28 (2)	71 (4)	7 (4)	36 (6)	2 (4)
C(1)	−505 (4)	2272 (3)	3,931 (5)	79 (5)	42 (3)	65 (5)	18 (6)	15 (9)	−12 (7)
C(2)	−189 (4)	1553 (4)	3,191 (5)	44 (4)	38 (3)	62 (5)	10 (6)	−13 (8)	−1 (7)
C(3)	−512 (5)	792 (4)	3,488 (5)	53 (4)	47 (4)	54 (5)	3 (7)	33 (8)	1 (7)
C(4)	−275 (4)	49 (4)	2,940 (5)	52 (4)	36 (3)	64 (5)	−2 (6)	−13 (8)	14 (7)
C(5)	−697 (4)	−727 (4)	3,443 (5)	71 (5)	40 (3)	76 (6)	−8 (7)	25 (8)	18 (7)
C(6)	2,965 (4)	1563 (4)	−1,943 (5)	69 (5)	37 (3)	85 (5)	−30 (6)	48 (9)	−5 (8)
C(7)	2,421 (4)	1017 (4)	−1,052 (5)	40 (4)	35 (3)	70 (5)	0 (5)	−11 (9)	−4 (7)
C(8)	2,467 (5)	195 (4)	−1,183 (5)	58 (4)	35 (3)	51 (5)	3 (6)	23 (9)	5 (7)
C(9)	1,999 (4)	−397 (4)	−464 (5)	49 (4)	31 (3)	64 (5)	11 (6)	−3 (8)	5 (7)
C(10)	2,155 (5)	−1287 (3)	−754 (5)	78 (5)	28 (3)	79 (6)	7 (6)	29 (9)	−1 (6)
H(1)	−908 (33)	755 (29)	4,035 (37)	2.16 (1.19)					
H(2)	2,760 (31)	7 (28)	−1,807 (37)	1.78 (1.17)					

[a] Values for the nickel atom have been multiplied by 10^5, those for other atoms by 10^4. Numbers in parentheses are estimated standard deviations in last significant figures. The anisotropic thermal parameter is defined as $\exp[-(\beta_{11}h^2 + \beta_{22}k^2 + \beta_{33}l^2 + \beta_{12}hk + \beta_{13}hl + \beta_{23}kl)]$. Isotropic thermal parameters, B, of the hydrogen atoms have the form $\exp[-B(\sin^2\theta/\lambda^2)]$.

Table III. Positional Parameters ($\times 10^4$) Generated for Methyl Group Hydrogen Atoms

	Atom	x	y	z
C(1)	H(3)	−183	2829	3573
	H(4)	−239	2186	4821
	H(5)	−1322	2320	3932
C(5)	H(6)	−445	−1244	2921
	H(7)	−1516	−701	3433
	H(8)	−436	−800	4337
C(6)	H(9)	2853	2201	−1712
	H(10)	2661	1451	−2811
	H(11)	3766	1424	−1937
C(10)	H(12)	1750	−1663	−126
	H(13)	2954	−1431	−717
	H(14)	1872	−1411	−1628

displaced such that the shortest intermolecular contacts are O1–O2′ and O1′–O2, 3.681 Å. The final positional and thermal parameters and their standard deviations for $Ni(TAA)_2$ are set out in Table II. The assumed atomic coordinates of the methyl hydrogen atoms are listed in Table III. Interatomic distances and angles are given in Table IV. Least-squares planes given in Table V indicate that the two chelate rings are very nearly planar, although the molecule as a whole is slightly twisted about its C_2 axis. There is a torsional angle of 4.5° between the two chelate rings.

The intraligand (SNiO) angles averaging 96.2 (1)° are considerably larger than the interligand SNiS and ONiO angles of 85.0 and 82.7°, respectively. The coordination asymmetry results in Ni–S–C and Ni–O–C angles of 110.8 and 133.8°, which may be compared with the Co–S–C angle of 117° in bis(dithioacetylace-

Table IV. Bond Distances and Bond Angles[a]

Atoms	Distance, Å	Atoms	Angle, deg
Ni–S(1)	2.142 (2)	S(1)–Ni–S(2)	85.0 (1)
Ni–S(2)	2.141 (2)	O(1)–Ni–O(2)	82.7 (2)
Ni–O(1)	1.883 (4)	S(1)–Ni–O(1)	96.3 (1)
Ni–O(2)	1.878 (4)	S(2)–Ni–O(2)	96.1 (1)
S(1)–C(2)	1.702 (6)	Ni–S(1)–C(2)	110.7 (2)
S(2)–C(7)	1.693 (6)	Ni–S(2)–C(7)	110.9 (2)
O(1)–C(4)	1.263 (7)	Ni–O(1)–C(4)	133.9 (4)
O(2)–C(9)	1.265 (7)	Ni–O(2)–C(9)	133.7 (4)
C(2)–C(3)	1.361 (9)	S(1)–C(2)–C(3)	126.2 (5)
C(7)–C(8)	1.358 (8)	S(2)–C(7)–C(8)	126.9 (5)
C(3)–C(4)	1.402 (9)	O(1)–C(4)–C(3)	125.4 (6)
C(8)–C(9)	1.410 (8)	O(2)–C(9)–C(8)	126.0 (5)
C(1)–C(2)	1.514 (8)	C(2)–C(3)–C(4)	127.5 (6)
C(6)–C(7)	1.536 (8)	C(7)–C(8)–C(9)	126.4 (6)
C(4)–C(5)	1.506 (8)	S(1)–C(2)–C(1)	114.5 (4)
C(9)–C(10)	1.515 (8)	S(2)–C(7)–C(6)	114.0 (4)
C(3)–H(1)	0.876 (43)	O(1)–C(4)–C(5)	115.8 (5)
C(8)–H(2)	0.932 (43)	O(2)–C(9)–C(10)	115.5 (5)
		C(1)–C(2)–C(3)	119.3 (5)
		C(6)–C(7)–C(8)	119.0 (5)
		C(3)–C(4)–C(5)	118.8 (5)
		C(8)–C(9)–C(10)	118.5 (5)
		C(2)–C(3)–H(1)	117.2 (3.2)
		C(7)–C(8)–H(2)	116.8 (2.8)
		C(4)–C(3)–H(1)	115.3 (3.2)
		C(9)–C(8)–H(2)	116.4 (2.8)

[a] Numbers in parentheses are estimated standard deviations in last significant figures.

Table V. Least-Squares Planes in Bis(monothioacetylacetonato)nickel(II)[a]

Atom	Dev (Å)	Atom	Dev (Å)
(1)	$0.7959X - 0.0644Y + 0.6020Z - 1.782 = 0$		
Ni	−0.0138	O(1)	−0.0558
S(1)	0.0542	O(2)	0.0632
S(2)	−0.0479		
(2)	$0.7956X - 0.1035Y + 0.5969Z - 1.714 = 0$		
Ni	0.0015	C(3)	−0.0033
S(1)	−0.0047	C(4)	−0.0014
C(2)	0.0064	O(1)	0.0014
(3)	$0.8034X - 0.0266Y + 0.5948Z - 1.831 = 0$		
Ni	−0.0172	C(8)	−0.0102
S(2)	0.0168	C(9)	0.0065
C(7)	−0.0063	O(2)	0.0103
(4)	$0.8005X - 0.0624Y + 0.5961Z - 1.786 = 0$		
Ni	−0.0168	C(4)	−0.0741
S(1)	0.0459	C(5)	−0.1004
S(2)	−0.0358	C(6)	−0.1182
O(1)	−0.0720	C(7)	−0.0327
O(2)	0.0654	C(8)	0.0115
C(1)	0.1303	C(9)	0.0659
C(2)	0.0354	C(10)	0.1246
C(3)	−0.0280		

[a] Planes were calculated using unit weight for all atoms.

The Ni–S and Ni–O distances of 2.14 and 1.88 Å, respectively, in $Ni(TAA)_2$ are normal for a square-planar, low-spin Ni(II) complex. For example, they closely resemble the corresponding bond lengths (Ni–S, 2.15, 2.18 Å; Ni–O, 1.86 Å) in the five-membered ring NiO_2S_2 chelate, bis(methylthiohydroxamato)nickel(II).[13] The S···S distance of 2.894 Å in $Ni(TAA)_2$ is relatively short, indicating favorable nonbonded interactions between sulfur atoms. Weak nonbonded S···S attractive forces thus could be responsible for the observed strong preference for cis stereochemistry in both bis and tris metal complexes of TAA, as has been suggested earlier.[4]

Infrared and Raman Spectra. The infrared spectrum of $Ni(TAA\text{-}d)_2$ exhibits bands at 882 and 673 cm^{-1} that were not reported[5] for the undeuterated compound (Table VI). Bands at 1338 and 815 cm^{-1} that were assigned[5] to $\delta(C\text{–}H) + \nu(C{\cdots}C)$ and $\pi(C\text{–}H)$ are much less intense in the deuterated complex. Analogous isotopic shifts in $Pt(acac)_2$[14] suggest that the 882- and 673-cm^{-1} bands are assignable to $\delta(C\text{–}D)$ and $\pi(C\text{–}D)$, respectively.

The far-infrared spectra of $Ni(TAA)_2$ and $Pd(TAA)_2$ are shown in Figure 3. Raman spectral data for both complexes are given in Table VI. Infrared and Raman bands between 700 and 300 cm^{-1} in $Ni(TAA)_2$ have virtually identical counterparts in $Pd(TAA)_2$. However, the pattern of bands below 300 cm^{-1} differs. In $Ni(TAA)_2$ there is a single intense ir band centered at 251 cm^{-1}, whereas the ir spectrum of $Pd(TAA)_2$ exhibits a weak shoulder at 266 cm^{-1}. The Raman spectrum of $Ni(TAA)_2$ exhibits an intense band at 194 cm^{-1} and a weaker band at 241 cm^{-1}. The most intense low-energy feature in the Raman spectrum of $Pd(TAA)_2$ is at 173 cm^{-1}, with weaker peaks at 250 and 228 cm^{-1}.

Table VI. Calculated and Observed Frequencies (cm^{-1}) for In-Plane Vibrations of Metal Monothioacetylacetonates

$Ni(TAA)_2$ Calcd A_1	$Ni(TAA)_2$ Calcd B_2	$Ni(TAA)_2$ Obsd Ir	$Ni(TAA)_2$ Obsd R	$Ni(TAA\text{-}d)_2$ Calcd A_1	$Ni(TAA\text{-}d)_2$ Calcd B_2	$Ni(TAA\text{-}d)_2$ Obsd Ir	$Pd(TAA)_2$ Calcd A_1	$Pd(TAA)_2$ Calcd B_2	$Pd(TAA)_2$ Obsd Ir	$Pd(TAA)_2$ Obsd R	Predominant modes
1571	1570	1564		1568	1567	1555	1581	1580	1568		$\nu(C{\cdots}O) + \nu(C{\cdots}C)_o$
1485	1484	1476		1462	1462	1473	1475	1475	1470		$\nu(C{\cdots}C)_s$
1300	1300	1338					1305	1305	1338		$\delta(C{—}H)$
1227	1227	1235, 1229		1251	1251	1235	1216	1216	1230		$\nu(C{\cdots}C)_o + \nu(C\text{–}CH_3)_o$
1130	1129	1118		1159	1159	1162	1116	1116	1113		$\nu(C\text{–}CH_3)_s$
				966	966	950					$\nu(C\text{–}CH_3)_o + \delta(C\text{–}D)$
922	920	937					925	923	928		$\nu(C\text{–}CH_3)_o$
				893	890	883					$\delta(C\text{–}D) + \nu(C\text{–}CH_3)_o$
743	742	721		705	704	705	717	716	718		$\nu(C{\cdots}S)$
653	647	642, 662	657	648	641	642, 662	640	638	656, 640	658	$\nu(M\text{–}O) + \delta(CCS) + \delta(CCO) + \delta(CCC)$ $\delta(C\text{–}CH_3)_o$
531		535	536	531		535	515		523	528	$\delta(CCS) + \delta(CCO) + \delta(CCC) + \delta(C\text{–}CH_3)_s$
	517	498, 492	495		517	498, 492		508	497, 493	496	$\delta(C\text{–}CH_3)_{s,o} + \delta(CCS) + \delta(CCO) + \delta(CCC)$
	420	410			420	410		396	405	408	$\delta(C\text{–}CH_3)_s + \nu(M\text{–}O)$
409		397	398	409		397	395		398, 393	396	$\delta(C\text{–}CH_3)_s + \nu(M\text{–}O)$
360	357	373		360	357	373	352	349	368		$\delta(CCS) + \delta(CCO)$
334				334			283		304	308	$\delta(CCS) + \delta(CCO) + \nu(M\text{–}S)$
	302	300			302	300		279			$\delta(C\text{–}CH_3)_o$
248		251	241	248		251	222		224	228	$\nu(M\text{–}S)$
	214		194		214			187		173	$\nu(M\text{–}S)$
	179				179			164	150		$\delta(MSC) + \delta(MOC) + \delta(SMO)$
131		113		131		113	132		100		$\delta(MSC) + \delta(MOC) + \delta(SMO)$
59		56		59		56	56		54		$\delta(SMS) + \delta(OMO)$

tonato)cobalt(II)[11] and the Ni–O–C angle of 127.1° in bis(2,2,6,6-tetramethylheptane-3,5-dionato)nickel(II).[12] The observed interatomic distances in the chelate ring are consistent with substantial delocalization of the π-bond framework. However, it is interesting that the C⋯C bond adjacent to C⋯S is slightly shorter than C⋯C next to C⋯O. It follows that C⋯O has more double bond character than C⋯S, which is to be expected. The fact that the C⋯O distance (1.26 Å) in $Ni(TAA)_2$ is shorter than the corresponding bond length (1.31 Å)[12] in bis(2,2,6,6-tetramethylheptane-3,5-dionato)nickel(II) supports this view.

(11) R. Beckett and B. F. Hoskins, *Chem. Commun.*, 909 (1967).
(12) F. A. Cotton and J. J. Wise, *Inorg. Chem.*, **5**, 1200 (1966).
(13) (a) T. Sato, K. Nagata, Y. Tsukuda, M. Shiro, and H. Koyama, *Chem. Commun.*, 215 (1967); (b) T. Sato, K. Nagata, M. Shiro, H. Koyama, *ibid.*, 192 (1966).
(14) G. T. Behnke and K. Nakamoto, *Inorg. Chem.*, **6**, 433 (1967).

The far-infrared and Raman spectra of $Zn(TAA)_2$ and $Cd(TAA)_2$ are also shown in Figure 3. Although the Zn(II) and Cd(II) complexes probably adopt a tetrahedral coordination geometry, their spectra should aid in unscrambling the metal–oxygen and metal–sulfur stretching vibrations in the planar chelates. Absorption bands located at 500, 365, 200, and 145 cm^{-1} remain comparatively invariant in the Zn(II) and Cd(II) chelates, whereas the bands at 640, 480, 400, and 259 cm^{-1} in $Zn(TAA)_2$ are shifted to 625, 450, 340, and 226 cm^{-1} in $Cd(TAA)_2$. Vibrations that have the largest metal–oxygen and metal–sulfur character are therefore found at 400 and 259 cm^{-1} in $Zn(TAA)_2$, and 340 and 226 cm^{-1} in $Cd(TAA)_2$.

Normal-Coordinate Analysis. As $Ni(TAA)_2$ has a cis planar structure, a 1 : 2 metal–ligand model possessing C_{2v} point symmetry was assumed. The methyl-group carbon and hydrogen atoms were treated as a single mass. Of the 45 possible normal vibrations, after excluding translations and rotations (16 A_1 + 7 A_2 + 7 B_1 + 15 B_2), only the 31 in-plane ones (16 A_1 + 15 B_2), which are both infrared and Raman active, were analyzed. The 17-atom model produced 44 internal (18 bond stretching and 26 angle bending) coordinates. Only 13 of the 26 angle bending coordinates are independent. Six redundancies comprised of the sum of three angles about each chelate-ring carbon atom and two redundancies involving the sum of six angles in the chelate rings were removed prior to solving the GF matrix for eigenvalues and eigenvectors. In addition, a high-frequency separation of the single C–H stretching frequency in each representation, A_1 and B_2, was performed. In C_{2v} symmetry the 34 remaining coordinates were divided into 18 A_1 and 16 B_2. The redundancies, 3 A_1 + 2 B_2, yielded zero frequencies in the eigenvalue problem. The GF matrix problem was solved by a procedure similar to the one described for monothioacetylacetonates[5] in the 1:1 metal–ligand model. Bending and repulsive force constants were transferred little changed from their previous values while stretching constants were varied by a least-squares procedure to fit the observed frequencies. The observed and calculated frequencies along with vibrational mode assignments are summarized in Table VI.

The A_1 and B_2 Ni–S stretching vibrations are calculated at 248 and 214 cm^{-1}, respectively, whereas the corresponding Pd–S frequencies are predicted at 222 and 187 cm^{-1}. The transition dipole moment is a maximum along the $C_2(y)$ axis for the symmetric M–S stretch and along the x axis for the asymmetric M–S stretch. An estimate of the values of $(\partial\mu_y/\partial Q_{13(A_1)})^2$ and $(\partial\mu_x/\partial Q_{13(B_2)})^2$ [μ_y and μ_x are the y and x components of the dipole moment; $Q_{13(A_1)}$ and $Q_{13(B_2)}$ are the normal coordinates associated with $\lambda_{13(A_1)}$ and $\lambda_{13(B_2)}$], which are proportional to the integrated band intensities,[15] indicates that

$$\left|\frac{\partial\mu_y}{\partial Q_{A_1}}\right| > \left|\frac{\partial\mu_x}{\partial Q_{B_2}}\right|$$

Therefore, most probably it is ν_s(M–S) that is observed as an intense infrared band at 251 cm^{-1} in $Ni(TAA)_2$ and at 224 cm^{-1} in $Pd(TAA)_2$. The asymmetric ν(M–S) apparently is not observed in the infrared and must be very weak. However, the intense Raman bands at 194 and 173 cm^{-1} in $Ni(TAA)_2$ and $Pd(TAA)_2$, respectively, are attributable to ν_{as}(M–S).

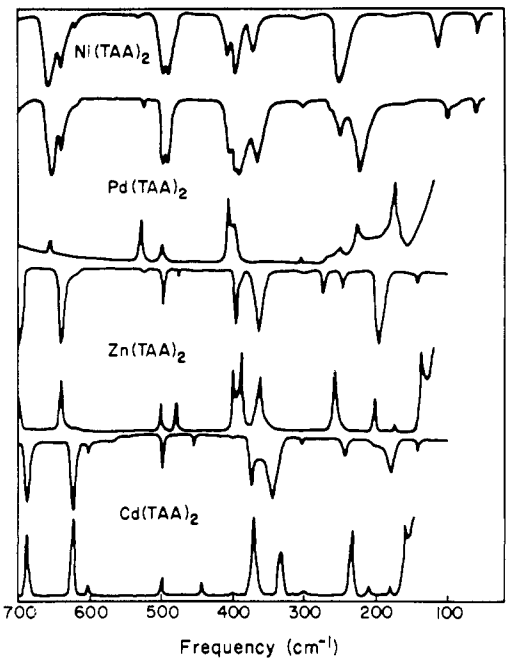

Figure 3. Infrared spectra of Nujol mulls of $Ni(TAA)_2$, $Pd(TAA)_2$, $Zn(TAA)_2$, and $Cd(TAA)_2$. Raman spectra of powdered solids of $Pd(TAA)_2$, $Zn(TAA)_2$, and $Cd(TAA)_2$.

The infrared and Raman spectra of $Zn(TAA)_2$ and $Cd(TAA)_2$ exhibit this same difference in intensities of infrared and Raman-active M–S stretching fundamentals. One species of ν(Zn–S) [ν(Cd–S)] is observed as a weak band at 273 [245] cm^{-1} in the infrared and as an intense band at 258 [236] cm^{-1} in the Raman. The other species is recorded as an intense band at 197 [180] cm^{-1} in the ir and as a medium intensity band at 204 [180] cm^{-1} in the Raman. The 245-cm^{-1} feature in the ir occurs in all cases and probably represents an out-of-plane ring mode.

Assuming tetrahedral coordination geometry, $Zn(TAA)_2$ would have C_2 point symmetry. As the C_2 axis lies between the SZnS and OZnO angles, the symmetric displacement of the sulfur atoms is along the same axis as in the cis planar geometry. Therefore, the intense ir band is expected to be ν_s(M–S) and the more intense Raman band should be ν_{as}(M–S). A normal-coordinate calculation for an approximately tetrahedral ZnO_2S_2 model having C_2 symmetry showed that ν_A(Zn–S) < ν_B(Zn–S), although the observed frequency difference is about twice as large as the one calculated.

The Ni–O and Pd–O stretching fundamentals are more difficult to locate, as there is little shift of the band frequencies between 700 and 300 cm^{-1} from $Ni(TAA)_2$ to $Pd(TAA)_2$. Bands between 400 and 350 cm^{-1} in $Zn(TAA)_2$ and $Cd(TAA)_2$ are the most sensitive to the nature of the metal atom. Metal isotopic shifts that have been observed in $Cu(acac)_2$ and $Pd(acac)_2$ are greatest for bands near 300 and 450 cm^{-1}, which were assigned to M–O stretching vibrations.[16] Although the normal-coordinate analysis predicts that the largest ν(Ni–O) [ν(Pd–O)] character occurs in bands near 650

(15) E. B. Wilson, J. C. Decius, and P. C. Cross, "Molecular Vibrations," McGraw-Hill, New York, N. Y., 1955, Chapter 7.

(16) K. Nakamoto, C. Udovich, and J. Takemoto, *J. Amer. Chem. Soc.*, **92**, 3973 (1970).

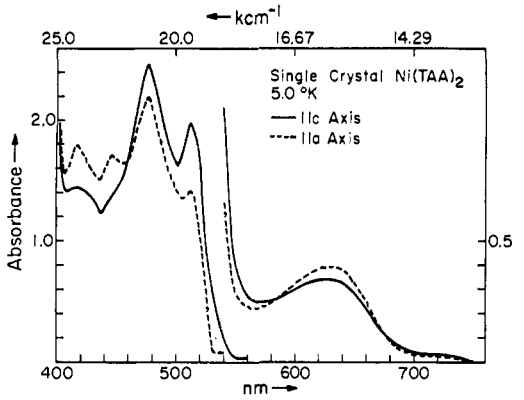

Figure 4. Polarized single-crystal electronic spectra of $Ni(TAA)_2$ at 5.0°K. Crystal thicknesses measured 3.6 (0.1) and 34 (2) μ for the left-hand and right-hand spectra, respectively.

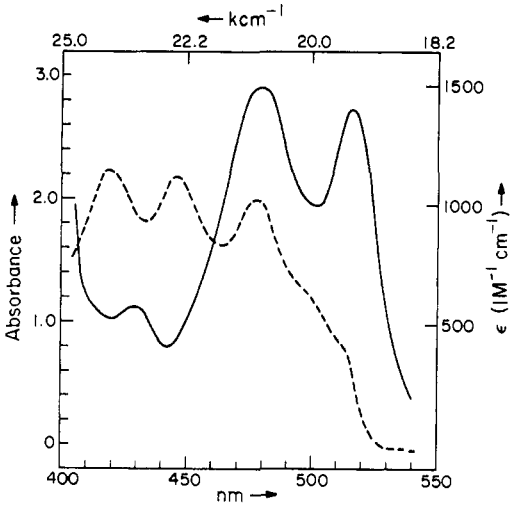

Figure 5. Calculated σ(——) and π(---) electronic spectra of $Ni(TAA)_2$.

cm^{-1}, it is more probable that M–O stretches contribute equally to bands near 650 and 400 cm^{-1}. Force constants which were varied in the analysis are set out in Table VII. Metal–sulfur stretching force constants,

Table VII. Force Constants (mdyn/Å)[a]

	$Ni(TAA)_2$	$Pd(TAA)_2$
K_1(C⋯S)	3.70	3.20
K_2(C⋯C)$_s$	4.90	4.00
K_3(C–CH_3)$_s$	3.40	3.30
K_4(M–S)	1.00	0.70
K_5(C⋯O)	7.00	7.40
K_7(M–O)	2.00	1.90
K_8(C⋯C)$_o$	5.10	4.80
K_9(C–CH_3)$_o$	3.70	3.80
H_5(CCH)	0.12	0.15
F_6(C···H)	0.45	0.48

[a] K, stretching; H, bending; F, repulsive.

K(Ni–S) = 1.00 and K(Pd–S) = 0.70 mdyn/Å, are more sensitive to the metal than metal–oxygen constants, K(Ni–O) = 2.00 and K(Pd–O) = 1.90 mdyn/Å. Thus, the reliability of the M–S constants is enhanced because of the far-infrared and Raman spectral data.

Electronic Spectra. The polarized absorption spectra between 750 and 400 nm for two single crystals of

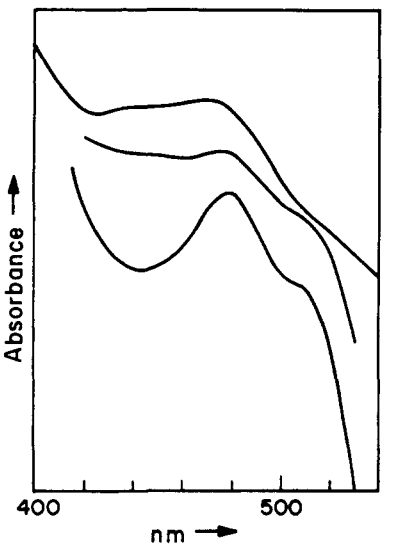

Figure 6. Thin film (deposited on quartz disk) electronic spectra of $Ni(TAA)_2$. The (010) crystal face increasingly predominates from top to bottom.

$Ni(TAA)_2$ at 5.0°K are shown in Figure 4. The thickness of the thin crystal (3.6 μ) was determined from interference band minima observed between 550 and 700 nm. Molecular coordinate axes were chosen such that z is perpendicular to the least-squares plane of Ni, S, O, and C atoms and y ($\equiv C_2$) bisects the S–Ni–S angle.

The direction cosines for the y axis are [(+0.1375, +0.9872, +0.0814), (+0.1375, +0.9871, −0.0814), (−0.1375, +0.9872, +0.0814), (−0.1375, +0.9872, −0.0814)]. Absorbance spectra along the extinction directions of the (010) crystal face, [001] and [100], will contain virtually no y component

$$A_c = 0.6381a_x + 0.0066a_y + 0.3553a_z$$
$$A_a = 0.3403a_x + 0.0189a_y + 0.6408a_z$$

The inverse matrix

$$\begin{pmatrix} a_\pi \\ a_\sigma \end{pmatrix} = \begin{pmatrix} -1.2581 & 2.2581 \\ 2.2445 & -1.2445 \end{pmatrix} \begin{pmatrix} A_c \\ A_a \end{pmatrix}$$

was used to transform the observed data into absorbances π (perpendicular to plane) and σ (in-plane).

The intensity (ϵ 80, methanol solution) of the broad band centered at 630 nm (15,870 cm^{-1}) suggests that one or more spin-allowed d–d transitions are involved. As the calculated π component of the 630-nm band is clearly dominant, the principal contributor to the intensity is most likely the z-allowed $^1A_1 \rightarrow {}^1B_1$ ($d_{xz} \rightarrow d_{xy}$). It is also probable that $^1A_1 \rightarrow {}^1A_2$ ($d_{yz} \rightarrow d_{xy}$), which is allowed only through vibronic coupling, and the x-allowed $^1A_1 \rightarrow {}^1B_2$ ($d_{x^2-y^2} \rightarrow d_{xy}$), lie in the same energy region and account for some of the σ intensity.

The 5°K σ and π crystal absorption spectra between 550 and 400 nm are shown in Figure 5. Band maxima are observed at 513 (19,490), 477 (20,960), and 428 nm (23,360 cm^{-1}) in σ polarization. The π spectrum exhibits significant peaks at 477 (20,960), 447 (22,370), and 418 nm (23,920 cm^{-1}).

A thin-film spectrum at 300°K in which random crystal orientations are present is shown in Figure 6. Changes in the film spectrum between 550 and 410 nm

as the [010] face becomes dominant are also shown. The broad band in the 450-nm region that develops in the film spectra appears weakly at 447 nm in the single-crystal spectrum. In methanol solution $Ni(TAA)_2$ exhibits a broad band at 445 nm ($\epsilon \sim 3300$) and a relatively weak shoulder at 500 nm ($\epsilon \sim 1160$).

We suggest that the absorption bands in the 550–400 nm region are attributable mainly to charge transfer transitions of the d → π^*L type. The bands are in the same general energy region and are similar in intensity to the assigned d → π^*L absorptions in several planar NiS_4 chelates.[17] In the D_{2h} complex $Ni(DTAA)_2$, where DTAA is dithioacetylacetonate, the lowest empty π^* levels have been calculated[17c] by semiempirical methods to be of a_u and b_{3g} symmetries. These two levels are nearly degenerate in $Ni(DTAA)_2$, being derived from the same π^*L orbital. Upon lowering the symmetry to C_{2v}, a_u and b_{3g} become a_2 and b_1, respectively. Using the well-established d → π^*L transition assignments[18-21] of $Ni(CN)_4^{2-}$ as a guide, it is reasonable to assume that b_1 will be the lowest π^* molecular orbital of $Ni(TAA)_2$, as in this case the sulfur $3p_\pi$ orbitals overlap and thereby derive stabilization from the empty metal $4p_z$ (b_1) orbital.

Let us now consider the interpretation of the most intense absorption features in the 550–400 nm region, represented by the bands at 477 and 447 nm, which are not well resolved from each other in the film and solution spectra. The band at 477 nm is $\sigma(x)$ polarized, and the suggested assignment is $^1A_1 \rightarrow {}^1B_2$ ($d_{xz} \rightarrow b_1\pi^*$). As neither A_c nor A_a contains a significant y component for the single crystal, the band at 447 nm, which intensifies in the film spectra, must be y polarized. Both y-allowed $^1A_1 \rightarrow {}^1A_1$ transitions, $d_{yz} \rightarrow b_1\pi^*$ and $d_{xz} \rightarrow a_2\pi^*$, probably contribute significantly to the 447-nm band intensity.

The band at 513 nm is strongly x polarized. We prefer to attribute this band to the x-allowed $^1A_1 \rightarrow {}^1B_2$ ($d_{z^2} \rightarrow d_{xy}$) transition, but assignment as a spin-forbidden d → $b_1\pi^*$ excitation which gains intensity from the nearby spin-allowed transition of $\sigma(x)$ polarization cannot be excluded. In the 5°K single-crystal spectrum the band at 418 nm appears in z polarization but is not resolved in either film or solution spectra. Assignment as the $^1A_1 \rightarrow {}^1B_1$ ($d_{x^2-y^2} \rightarrow b_1\pi^*$) charge transfer transition is reasonable from energy and intensity considerations. This transition would be expected to be allowed weakly in z polarization only. The weak x-polarized feature at 428 nm can be tentatively assigned as the x-allowed transition $^1A_1 \rightarrow {}^1B_2$ ($d_{yz} \rightarrow a_2\pi^*$).

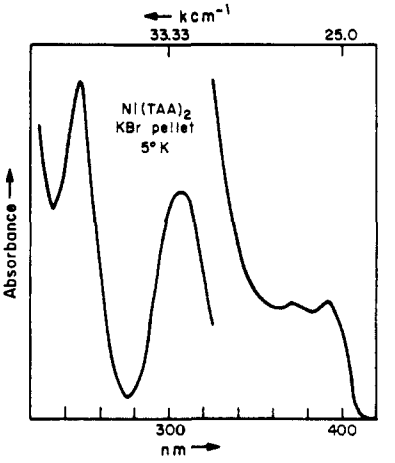

Figure 7. Electronic spectrum of $Ni(TAA)_2$ at 5.0°K in a KBr pellet.

A potassium bromide pellet spectrum of $Ni(TAA)_2$ at 5.0°K between 410 and 220 nm is shown in Figure 7. The broad band observed at 383 nm in chloroform solution[2] is resolved into bands at 390 and 370 nm in the 5°K spectrum. The intense bands observed below 410 nm are undoubtedly due to a combination L(π) → L(π^*) and charge transfer transitions, but without additional data more detailed assignment is not possible.

Acknowledgments. We thank Drs. A. J. Frueh and R. E. Marsh for helpful discussions on aspects of X-ray crystallography. O. S. thanks the National Research Council of Canada for a postdoctoral Fellowship (1970–1972). This research was supported by the National Science Foundation and the National Research Council of Canada.

Supplementary Material Available. A listing of structure factor amplitudes will appear following these pages in the microfilm edition of this volume of the journal. Photocopies of the supplementary material from this paper only or microfiche (105 × 148 mm, 24× reduction, negatives) containing all of the supplementary material for the papers in this issue may be obtained from the Journals Department, American Chemical Society, 1155 16th St., N.W., Washington, D. C. 20036. Remit check or money order for $3.00 for photocopy or $2.00 for microfiche, referring to code number JACS-74-2353.

(17) (a) A. R. Latham, V. C. Hascall, and H. B. Gray, *Inorg. Chem.*, **4**, 788 (1965); (b) S. I. Shupack, E. Billig, R. J. H. Clark, R. Williams, and H. B. Gray, *J. Amer. Chem. Soc.*, **86**, 4594 (1964); (c) O. Siiman and J. Fresco, *ibid.*, **92**, 2652 (1970); (d) R. Dingle, *Inorg. Chem.*, **10**, 1141 (1971).

(18) In $Ni(CN)_4^{2-}$ the assignment[19a] of the low-energy charge transfer spectrum as due to transitions to a $4p_z$-stabilized π^*CN orbital has been fully confirmed by polarized-single-crystal absorption[19c] and MCD[20] spectral experiments, as well as by *ab initio* SCF-LCAO-MO calculations.[21]

(19) (a) H. B. Gray and C. J. Ballhausen, *J. Amer. Chem. Soc.*, **85**, 260 (1963); (b) W. R. Mason and H. B. Gray, *J. Amer. Chem. Soc.*, **90**, 5791 (1968); (c) C. D. Cowman, C. J. Ballhausen, and H. B. Gray, *ibid.*, **95**, 7873 (1973).

(20) (a) P. J. Stephens, A. J. McCaffery, and P. N. Schatz, *Inorg. Chem.*, **7**, 1923 (1968); (b) S. P. Piepho, P. N. Schatz, and A. J. McCaffery, *J. Amer. Chem. Soc.*, **91**, 5994 (1969).

(21) (a) J. Demuynck, A. Veillard, and G. Vinot, *Chem. Phys. Lett.*, **10**, 522 (1971); (b) J. Demuynck and A. Veillard, *Theor. Chim. Acta*, **28**, 241 (1973).